



## Influence of CO addition on the toluene total oxidation over Co based mixed oxide catalysts



Eric Genty<sup>a,\*</sup>, Julien Brunet<sup>a</sup>, Christophe Poupin<sup>a</sup>, Satu Ojala<sup>b</sup>, Stéphane Siffert<sup>a</sup>, Renaud Cousin<sup>a,\*</sup>

<sup>a</sup> Université du Littoral Côte d'Opale, Unité de Chimie Environnementale et Interactions sur le Vivant (UCEIV), 145 Avenue Maurice Schumann, 59140, Dunkerque, France

<sup>b</sup> University of Oulu, Environmental and Chemical Engineering, POB 4300, 90014, University of Oulu, Finland

### ARTICLE INFO

#### Keywords:

Mixed oxide  
Cerium  
Cobalt  
CO - toluene  
Catalytic oxidation

### ABSTRACT

Hydrotalcite like compounds containing Co, Al and Ce were synthesized by co-precipitation. The mixed oxides obtained after calcination were characterized by several techniques: XRD, BET, H<sub>2</sub>-TPR and XPS. Activities of mixed oxides were evaluated in toluene total oxidation in presence or in absence of carbon monoxide. The benzene, benzyl alcohol and benzaldehyde are principal by-products observed during toluene oxidation in presence of CoAl(Ce) mixed oxides. Moreover, presence of carbon monoxide improves toluene total oxidation over CoAlCe mixed oxides. Stability of the two best catalytic materials has been tested in the two conditions and show no deactivation.

### 1. Introduction

During the last decades, environmental legislation has imposed increasingly stringent targets for the permitted levels of atmospheric emissions. Volatile Organic Compounds (VOCs), as one of the main atmospheric pollutants, are released to the atmosphere from a variety of sources, such as automobile exhaust, petrochemical processes and from the treatment of the solid and liquid wastes. These regulations have induced the development of different methods for elimination [1–3]. The destructive methods transform VOCs into other compounds, inert or less dangerous. Catalytic total oxidation is a technique in which pollutants are oxidized completely (into carbon dioxide and water molecules) in presence of a catalytic material. It has the advantages to not generate NOx and to provide nearly total elimination of pollutants, with lower generation of organic by-products at moderate temperatures (approximately 300 °C), hence with low operation cost. VOC destruction processes are applied often to pollutants at low concentration, so that oxidation require external heating. In these cases, working at low temperature is important in order to improve the economy of the process. For this reason, an active and selective catalyst is required [1].

There are two types of catalysts used in these processes: oxides of transition metals (Co, Cu, Mn,...) and supported noble metals (Pt, Pd, Rh, ...). It is generally admitted that noble metal catalysts are preferred when there are no poisons (such as sulfur compounds, carbon monoxide...) present, and aromatic compounds are involved in the reaction.

However, due to the high cost of the noble metals, many studies have been devoted to the development of suitable catalysts containing only transition metal oxides [4–10]. Hydrotalcite-like compounds (HT) are presented as precursors of mixed oxides, with an enormous potential for the generation of well dispersed, active and very stable catalyst for several applications [11–13]. Mixed oxides are formed with calcination of HT structure, which possess unique properties such as high surface area and porosity, good thermal stability, homogeneous mixed oxide, basicity and high metal cation dispersion [14,15].

The application of mixed oxides as catalyst in the environmental field is very important. For example, the mixed oxides are active and selective for the decomposition of nitrogen oxides [16] or for the VOCs total oxidation [11,16]. The mixed oxides are used equally as catalysts [12,17,18] or as catalytic supports [16,17,19] in redox reactions such as in the total or selective oxidation of hydrocarbons, of VOCs and CO [12,13,18,20]. The mixed oxides containing cobalt and aluminum prepared from the hydrotalcite precursor show a good catalytic activity for the VOC total oxidation [18,20,21]. The key determining factors in the activity of cobalt oxides are the nature and distribution of these species on the surface [22,23]. The preparation methods, the nature of the support and the precursors and the metal loading influence the state of cobalt oxide species [24–26]. The use of metallic oxides with promoters that are composed of earth elements can lead to an improvement in the oxygen storage capacity, which evidently enhances the oxidation reaction [6,7].

\* Corresponding authors.

E-mail addresses: [eric.genty@univ-littoral.fr](mailto:eric.genty@univ-littoral.fr) (E. Genty), [Renaud.Cousin@univ-littoral.fr](mailto:Renaud.Cousin@univ-littoral.fr) (R. Cousin).

In a previous work [27], we have studied the behavior of Co-Al catalysts prepared by several methods (microwaves (MW), ultrasound (US) and conventional co-precipitation (CT)). In this study, we observed the enhancement of the reducibility and activity in the toluene total oxidation with catalysts prepared by non-conventional methods. The catalyst prepared by MW synthesis presented the best activity. In another work [28], we showed the influence of the partial replacement of  $\text{Al}^{3+}$  of the hydrotalcite structure by  $\text{Ce}^{3+}$  cation on the toluene oxidation. The presence of Ce in the mixed oxide improves the reducibility of the catalyst and thereby the toluene oxidation activity compared with the catalyst without cerium.

In the present study, we decided to investigate the activity of three samples showing the best catalytic activity in previous work i.e. the Co-Al mixed oxide prepared by conventional co-precipitation method with and without addition of cerium [28,29]. The main novelty objective of this work is to evaluate the influence of the carbon monoxide on the toluene total oxidation. Indeed, studies of the VOC oxidation, especially toluene, have been widely reported in the literature [9,29,30–32]. However, studies on the simultaneous catalytic oxidation of toluene and CO compounds in a mixture are very limited, even though this is an important step towards industrial environmental applications. Thus, the mixed oxides were analyzed by several physico-chemical techniques such as X-Ray Diffraction (XRD), X-Ray Photoelectron Spectroscopy (XPS),  $\text{H}_2$  Temperature Programmed Reduction ( $\text{H}_2\text{-TPR}$ ) allowing to understand in more details the influence of these physico-chemical characters on the toluene conversion with or without CO in the effluent.

## 2. Experimental

### 2.1. Preparation of catalysts

The reference catalysts were prepared by co-precipitation method described also in previous work [27,28]. An aqueous solution of 200 mL was prepared with appropriate amounts of  $\text{Co}(\text{NO}_3)_2 \cdot 6\text{H}_2\text{O}$ ,  $\text{Al}(\text{NO}_3)_3 \cdot 9\text{H}_2\text{O}$  with a molar ratio of  $\text{Co}^{2+}/\text{Al}^{3+}$  of 6/2 (solution A). This solution was added drop by drop to 300 mL of a  $\text{Na}_2\text{CO}_3$  solution (1 mol L<sup>-1</sup>, solution B). The pH of the solution was maintained at 10.5 with a NaOH solution (2 mol L<sup>-1</sup>). After addition, the suspension was stirred for 24 h at room temperature. Then, the suspension was filtered and washed with warm deionized water (60 °C). The solid obtained was dried in an oven for 64 h at 60 °C before grinding. The hydrotalcite intermediate was named as CoAlO. The same methodology was used for the synthesis of CoAlCeO following a similar molar ratio ( $\text{M}^{2+}/\text{M}^{3+} = 3$ ) and using in the solution A, a cerium nitrate ( $\text{Ce}(\text{NO}_3)_3 \cdot 6\text{H}_2\text{O}$ ) as the source of cerium.

The second synthesis method used was the co-precipitation assisted by microwave irradiation [27]. Sample was prepared by mixing sodium hydroxide (NaOH, 2 mol L<sup>-1</sup>) and sodium carbonate ( $\text{Na}_2\text{CO}_3$ , 1 mol L<sup>-1</sup>) in aqueous solution (100 mL) containing appropriate amounts of metal nitrates ( $\text{Co}(\text{NO}_3)_2 \cdot 6\text{H}_2\text{O}$  and  $\text{Al}(\text{NO}_3)_3 \cdot 9\text{H}_2\text{O}$ ). The metal salt solution was then added dropwise to 200 mL of deionized water maintained at a pH of 10.5 with NaOH aqueous solution (2 mol L<sup>-1</sup>). Next the solution was placed in a reactor inserted in a single mode microwave furnace (type Synthewave Prolabo 402 (300 W)) with mechanical agitation and a temperature control by infrared pyrometer for one hour at 80 °C. No pH change was observed during the maturation phase. After the precipitate was filtered and washed until pH was 7. Then, the solid was dried at 60 °C for 64 h. The sample was named as CoAlOMW (where MW corresponds to the hydrotalcite preparation using microwaves).

To obtain the mixed metal oxides, a thermal treatment was performed under flow of air (4 L h<sup>-1</sup>, 1 °C min<sup>-1</sup>, 4 h at 500 °C). The calcined samples were named as CoAlO, CoAlOMW and CoAlCeO.

Cerium hydroxide  $\text{Ce}(\text{OH})_4$  was precipitated from cerium(III) nitrate hexahydrated solution ( $\text{Ce}(\text{NO}_3)_3 \cdot 6\text{H}_2\text{O}$ ) with a sodium hydroxide solution (NaOH). The resulting hydroxides mixture was filtered,

washed, and dried overnight at 100 °C, before calcination under air flow (4 L h<sup>-1</sup>) at 400 °C (1 °C min<sup>-1</sup>) for 4 h to obtain ceria  $\text{CeO}_2$ .

A sample of  $\text{Co}_3\text{O}_4$  was prepared from  $\text{Co}(\text{NO}_3)_2 \cdot 6\text{H}_2\text{O}$  via precipitation by NaOH, and then calcined at 300 and 500 °C. The cobalt hydroxide was filtered, washed, and dried overnight at 100 °C, before calcination under air flow (4 L h<sup>-1</sup>) at 400 °C (1 °C min<sup>-1</sup>) for 4 h to obtain ceria  $\text{Co}_3\text{O}_4$ .

### 2.2. Characterization techniques

The specific surface areas of solids were determined by the BET method using a QSurf M1 apparatus (Thermoelectron), and the  $\text{N}_2$  adsorption at -196 °C.

Crystallinity of solids was determined at room temperature by X-Ray Diffraction (XRD) technique with a Bruker D8 Advance diffractometer equipped with a copper anode ( $\lambda = 1.5406 \text{ \AA}$ ) and a LynxEye Detector. The scattering intensities were measured over an angular range of  $10^\circ \leq 2\theta \leq 80^\circ$  for all samples with a step-size of  $\Delta(2\theta) = 0.02^\circ$  and a count time of 4 s per step. The diffraction patterns were indexed by comparison with the "Joint Committee on Powder Diffraction Standards" (JCPDS) files.

Temperature-Programmed Reduction ( $\text{H}_2\text{-TPR}$ ) experiments were carried out in an Altamira AMI-200 apparatus. Prior to the TPR experiment, 30 mg sample was treated under argon at 150 °C for 1 h. The samples were then heated from ambient temperature to 900 °C under  $\text{H}_2$  flow (5%vol. in argon – 30 mL min<sup>-1</sup>) with a heating rate of 5 °C min<sup>-1</sup>.

X-ray photoelectron spectroscopy (XPS) analyses were conducted with Kratos Axis Ultra DLD spectrometer with a monochromatic Al K $\alpha$  ( $h\nu = 1486.6 \text{ eV}$ ) radiation source operated at 15 kV and 15 mA. The binding energy (BE) was calibrated based on the line position of C 1s (285 eV). CasaXPS processing software was used to estimate the relative abundance of the different species.

Elemental compositions of samples were analysed using an iCAP-6300-DUO ICP-OES (Thermo Electron). 50.0 mg of powder were dissolved in 5 mL of aqua regia ( $\text{HNO}_3/\text{HCl}$  1:2) under microwave during 30 min (model MARSXpress, CEM). The solution was diluted extended to 50.0 mL with ultrapure water, and then diluted to 10% and filtered with a 0.45  $\mu\text{m}$  cellulosic micro-filter.

### 2.3. Catalytic tests

The activities of the catalysts (100 mg) were evaluated in total oxidation of toluene. The reactor was operated at continuous flow with a fixed bed catalyst at atmospheric pressure. Before each test, the catalyst was activated under flowing air (2 L h<sup>-1</sup>) at 500 °C for 4 h. The flow of the reactant gases (100 mL min<sup>-1</sup> with 1000 ppm of  $\text{C}_7\text{H}_8$  and 20%  $\text{O}_2$  in He) was adjusted by a Michell apparatus consisting of a saturator and mass flow controllers. After reaching a stable flow, reactants were passed through the catalyst bed and the temperature was increased from room temperature to 400 °C (1 °C min<sup>-1</sup>). The feed and the reactor outflow gases were analysed on line by a micro-gas chromatograph (Agilent 490 Micro gas chromatography) and infrared analysers (ADEV 4400 IR). The catalysts' performance was assessed in terms of  $T_{50}$ , defined as the temperature, when 50% conversion was obtained.

The toluene conversion was calculated taken into account the products and by-products and as a function of carbon number for each compound:

$$X_T = \left( \frac{[\text{CO}_2]_T + [\text{CO}]_T + [\text{C}_6\text{H}_6]_T * 6}{[\text{CO}_2]_T + [\text{CO}]_T + [\text{C}_6\text{H}_6]_T * 6 + [\text{C}_7\text{H}_8]_T * 7} \right) * 100 \quad (1)$$

Where:

- $X_T$  is the toluene conversion at the  $T$  temperature (%);
- $[I]_T$  is the concentration of the compound  $I$  at the  $T$  temperature (ppm).

The activity of the catalysts (100 mg) in toluene total oxidation in presence of CO was studied with the same experimental set-up. The experimental procedure used was the same as before except the flow of the reactant gases used was  $100 \text{ mL min}^{-1}$  with 1000 ppm of  $\text{C}_7\text{H}_8$ , 1000 ppm CO and 20%O<sub>2</sub> in He.

The toluene conversion was calculated taken into account the products and by-products (except the CO due to the presence in the gaseous flow) and as a function of carbon number for each compound:

$$X_{TolT} = \left( \frac{([CO_2]_{AnaT} - [CO_2]_{COT}) + 6 * [C_6H_6]_T}{([CO_2]_{AnaT} - [CO_2]_{COT}) + 6 * [C_6H_6]_T + 7 * [C_7H_8]_T} \right) \quad (2)$$

Where:

- $X_{TolT}$  is the toluene conversion at the  $T$  temperature (%);
- $[I]_T$  is the concentration of the compound  $I$  at the  $T$  temperature (ppm).

-  $[CO_2]_{AnaT} - [CO_2]_{COT}$  is the  $\text{CO}_2$  concentration issued from the toluene conversion and calculated with the following relationship:

$$[CO]_0 - [CO]_{Ana} = [CO]_{con} = [CO_2]_{COT} \quad (3)$$

Where:

- $[CO]_{con}$  is the concentration of CO converted at T temperature (ppm)
- $[CO]_0$  is the initial CO concentration (ppm)
- $[CO]_{Ana}$  is the CO concentration observed on the analyser (ppm)
- $[CO_2]_{COT}$  is  $\text{CO}_2$  concentration issued from the CO oxidation (ppm)

### 3. Results and discussion

#### 3.1. Total oxidation of toluene

The catalytic performance of the three samples for total oxidation of toluene is represented in Fig. 1. The catalytic behaviour is compared to the  $\text{Co}_3\text{O}_4$  and  $\text{CeO}_2$  samples.

The catalytic activity according to the  $T_{50}$  values follows this order (Table 1):



A better activity is observed for the solid containing cerium species compared to the other two solids. Moreover, the catalyst prepared by using microwaves shows a better reactivity compared to the conventional catalyst. The CoAlCeO and CoAlOMW catalysts show a total conversion of toluene at lower temperature than the  $\text{Co}_3\text{O}_4$  and  $\text{CeO}_2$

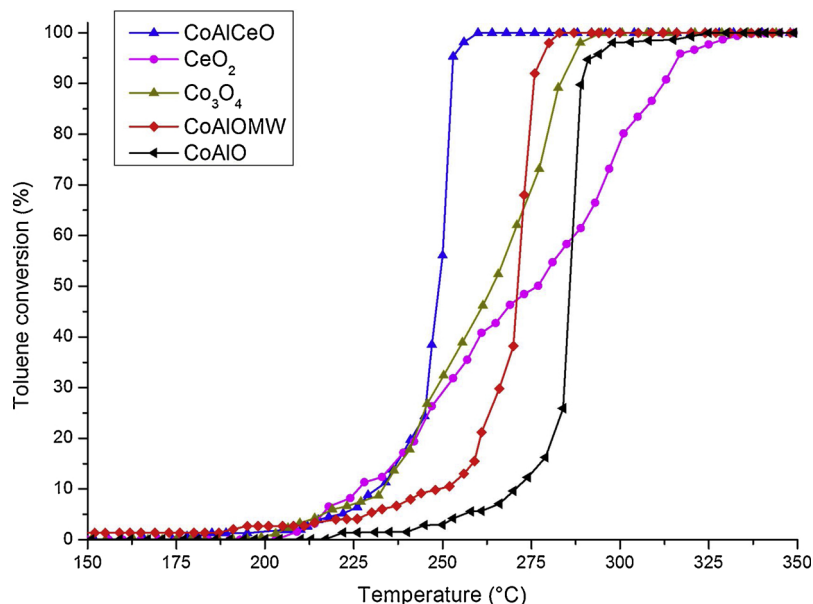


Fig. 1. Conversion of toluene (percentage) on mixed oxides vs. reaction temperature (°C).

catalysts. Concerning the toluene oxidation reaction, when the conversion is complete,  $\text{H}_2\text{O}$  and  $\text{CO}_2$  are the only products observed. However, during the toluene conversion over all the samples, quantitative amounts of benzene (around 2 ppm maximum for all mixed oxides) and CO (200 ppm for CoAlO, 125 ppm for CoAlOMW and 20 ppm for CoAlCeO) are observed. In addition, trace amounts of other by-products such as benzaldehyde, furan, benzyl alcohol and alkane compounds (methane, ethane) are detected as well. The by-products analysis will be presented in more detail in the Section 3.4.

#### 3.2. Physicochemical characterisations of mixed oxides

To understand the catalytic behaviour of the materials, physicochemical characterisations were done. The results of the dried samples have been already published in two previous articles, that is the reason why this document is focused on the mixed oxides only [28,29]. The textural properties of the solids and the chemical composition of mixed oxides are reported in the Table 2. In the first step, to investigate the crystalline structure of the samples, X-Ray Diffraction analyses were performed.

The diffractograms shown in Fig. 2, suggest the presence of three spinel phases whose diffraction lines are superimposed. Concerning the solids without cerium species, three spinel phases are observed the spinel phase of cobalt (II) and cobalt (III) ( $\text{Co}_3\text{O}_4$  (JCPDS-ICDD 42-1467)) and cobalt-aluminum spinel  $\text{CoAl}_2\text{O}_4$  phases (JCPDS-ICDD 44-0160) and  $\text{Co}_2\text{AlO}_4$  (JCPDS-ICDD 38-0814). The presence of the first phase ( $\text{Co}_3\text{O}_4$ ) is due to the easy oxidation of  $\text{Co}^{2+}$  to  $\text{Co}^{3+}$  in contact with oxygen and the greater thermodynamic stability of this phase compared to  $\text{CoO}$  [33]. However, the three diffraction lines of these three spinels are close in position ( $2\theta$ ) and in intensity [27]. For this reason, the crystalline phase cannot be identified by XRD. Concerning the solid with Ce, a fourth phase is observed which corresponds to ceria ( $\text{CeO}_2$  JCPDS-ICDD 34-0394).

In H<sub>2</sub>-TPR analysis of mixed oxide Co-Al (Fig. 3), two reduction zones are observed: one at less than 400 °C and another at a higher temperature ( $T > 400$  °C). The first zone (330 °C) corresponds to the reduction of  $\text{Co}_3\text{O}_4$  species into metallic cobalt ( $\text{Co}^\circ$ ), confirmed by the H<sub>2</sub>-TPR analysis of  $\text{Co}_3\text{O}_4$  sample. The second zone corresponds to the reduction of cobalt-aluminum spinel species ( $\text{CoAl}_2\text{O}_4$  or  $\text{Co}_2\text{AlO}_4$ ) into  $\text{Co}^\circ$  [27].

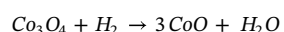


**Table 1**

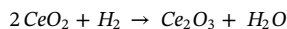
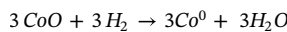
$H_2$  consumption from  $H_2$ -TPR and XPS data of CoAl(Ce)O issued from different preparation methods.

Mixed oxides	$H_2$ consumption (mmol. g <sup>-1</sup> )		Surface content (%) by XPS		$T_{50}$ for the toluene conversion (°C)	$T_{50}$ for the toluene conversion (°C)
	T < 400 °C	Total	O <sub>II</sub> /O <sub>I</sub>	Co <sup>2+</sup> /Co <sup>3+</sup>		
CoAlO	2.65	11.7	0.86	2.38	287	263
CoAlOMW	2.86	11.9	1.05	2.98	271	247
CoAlCeO	2.99	12.4	1.27	2.89	248	222

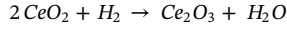
**Table 2**

Summary of the physicochemical properties for the mixed oxides.

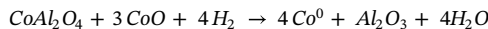
Mixed oxides	S <sub>BET</sub> (m <sup>2</sup> /g)	Pore Volume (cm <sup>3</sup> /g)	Pore Diameter (nm)	Atomic ratio Co/Al/Ce
CoAlO	123	0.21	7.5	6.0/2.1/0
CoAlOMW	167	0.48	6.3	6.0/2.0/0
CoAlCeO	108	0.10	3.7	6.0/1.22/0.73



The solid containing cerium has also two reduction zones ( $T < 400$  °C and  $T > 400$  °C). The first step is composed of three stages of reduction corresponding to the reduction of  $Co_3O_4$  into Co<sup>0</sup> and  $CeO_2$  surface species into  $Ce_2O_3$  according to following reactions:



The second step of reduction is related to the reduction of the spinel phases ( $CoAl_2O_4$  and  $Co_2AlO_4$ ) and ceria present in the catalyst bulk (bulk  $CeO_2$ ) following the chemical reactions:



The  $H_2$  consumption in the temperature range corresponding to the catalytic activity in toluene oxidation ( $T < 400$  °C) and for the overall  $H_2$ -TPR analysis are reported in Table 1. Reduction of ceria containing catalysts starts at lower temperature compared to the other two catalysts; this could be due to the interaction between the Ce and Co atoms. Moreover, the  $H_2$  consumption is higher in case of the CoAlCeO. The reducibility order according to the  $H_2$  consumption at lower

temperature ( $T < 400$  °C) is following the same order than the catalytic activity order observed for the toluene total oxidation. A relationship between the low-temperature reducibility and the toluene conversion suggests that the active phase of the catalyst corresponds to a  $Co_3O_4$  and a redox mechanism for this reaction can be suggested, which was confirmed in a previous paper [30]. This mechanism called also as Mars Van-Krevelen mechanism, is reported also in the bibliography for the total oxidation of VOC in presence of metal oxide catalysts [8,27,34].

The three CoAl(Ce)O catalysts were also investigated by XPS to examine the influence of the preparation method on the nature and the oxidation degree of surface species. The XPS spectra of O 1s and Co 2p are shown in Fig. 4, and the XPS data are summarized in Table 1. Regarding the oxygen 1s photopeak (O 1s), three components are observed. The first component (O<sub>III</sub>) at 533–534 eV corresponds to the oxygen present in the form of adsorbed carbonates or adsorbed water molecules [34]. The second component (O<sub>II</sub>) at 531 eV corresponds to adsorbed surface oxygen ( $O_2^-$  or  $O^-$ ) or hydroxyl groups ( $HO^-$ ) [35,36]. The last one (O<sub>I</sub>) which is located at a lower binding energy is consistent with the bulk type oxygen  $O^{2-}$ . The oxygen composition on the surface of the solid plays an important role in the catalytic activity of the oxidation reactions. Indeed, O<sub>II</sub> species exhibit greater mobility than the oxygen in the solid structure. In addition, several authors [35,36] have shown that the catalytic activity of the solid could be correlated to the presence larger amount of O<sub>II</sub> species. A ratio between O<sub>I</sub> and O<sub>II</sub> species are calculated for all samples (Table 1). It was revealed that for CoAlOMW and CoAlCeO, the ratio O<sub>II</sub>/O<sub>I</sub> is higher than that for the conventional CoAlO catalyst

Concerning the cobalt species, overlay photopeaks corresponding to Co 2p are represented on Fig. 4b. The profile observed is characteristic for materials consisting of a mixture of Co<sup>2+</sup> and Co<sup>3+</sup> ( $CoAl_2O_4$  or  $Co_3O_4$ ) [34,37]. This mixture of cobalt species (Co<sup>2+</sup> and Co<sup>3+</sup>) is verified by measuring the AE corresponding to the difference of bonding energy between Co 2p<sub>3/2</sub> and Co 2p<sub>1/2</sub> (Table 1). A value of

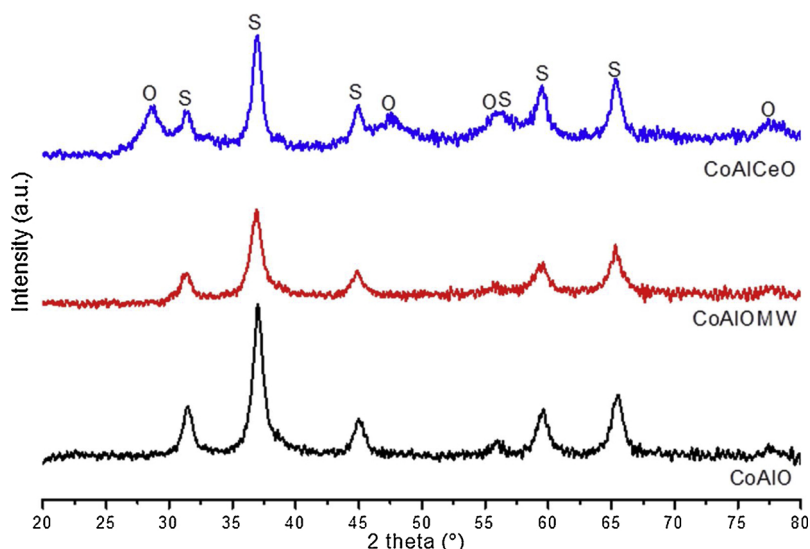
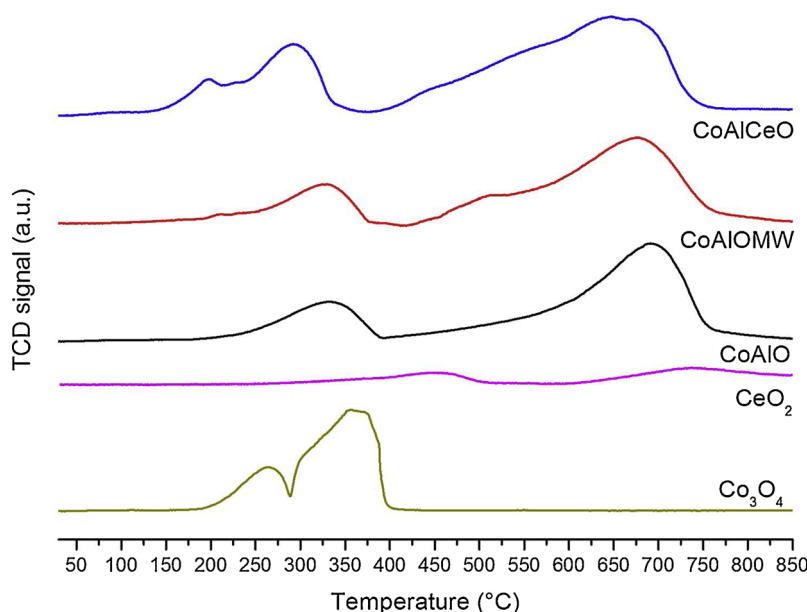


Fig. 2. X-Ray diffraction patterns for the mixed oxides (S:  $Co_3O_4$ ,  $CoAl_2O_4$  and  $Co_2AlO_4$ , o:  $CeO_2$ ).



**Fig. 3.**  $\text{H}_2\text{-TPR}$  profiles of the mixed oxides.

this  $\Delta E$  equals to 16 eV corresponds to the presence of only cobalt as  $\text{Co}^{2+}$  species and while a value equals to 15 eV is associated with the presence of only  $\text{Co}^{3+}$  [38]. For CoAlO, this value is equal to  $\Delta E$  15.2 eV, which shows that surface has both  $\text{Co}^{3+}$  and  $\text{Co}^{2+}$ . Then, in the case of the mixed oxide prepared using microwaves,  $\Delta E$  is equal to 15.4 eV. The higher  $\Delta E$  value for this catalyst suggests that the  $\text{Co}^{2+}$  amount on the surface is higher in this catalyst than on the other catalysts.

The relationship between  $\text{Co}^{2+}$  and  $\text{Co}^{3+}$  species (Table 1) is also calculated as the ratio of the area of the  $\text{Co}^{2+}$  signal component  $\text{Co } 2p_{3/2}$  and that of  $\text{Co}^{3+}$  signal component  $\text{Co } 2p_{3/2}$  described in detail in literature [34,38]. The proportion of  $\text{Co}^{2+}$  on the surface confirms the presence of the oxygen vacancy or  $\text{O}_{\text{II}}$  species for the CoAlCeO and CoAlOMW higher than for CoAlO mixed oxide. Indeed, Fig. 5 shows the relationship between the proportion of  $\text{O}_{\text{II}}/\text{O}_{\text{I}}$  obtained with the XPS and the catalytic activity measured at 241 °C corresponding to the toluene conversion equal to 20% for CoAlCeO catalyst. This relationship shows that the high proportion of  $\text{O}_{\text{II}}$  species results in higher catalyst activity that can be explained by the higher mobility of the adsorbed oxygen species compared to the bulk oxygen species. It have been already observed that for this type of catalytic materials, the  $\text{Co}_3\text{O}_4$  is the principal active phase for toluene total oxidation [27,28,30]. Moreover, the high quantity of oxygen adsorbed due to the presence ceria on the material, and the presence of  $\text{Co}_3\text{O}_4$  active phase create a synergistic effect to increase the reducibility of the materials that allow obtaining an active catalyst for the oxidation of toluene at low temperature.

### 3.3. Total oxidation of Toluene in presence of CO in reactional mixture

The catalytic performance of the three samples for toluene total oxidation in presence of CO or not is represented in Fig. 6. The catalytic activity according to the toluene  $T_{50}$  values in both cases follows the order

$$\begin{aligned} \text{CoAlCeO (mixture)} &> \text{CoAlCeO} = \text{CoAlOMW (mixture)} > \text{CoAlOMW} \\ &> \text{CoAlO (mixture)} > \text{CoAlO} \end{aligned}$$

An increase in the catalytic activity for the toluene total oxidation in presence of CO was observed for all solids. The  $T_{50}$  decreased by approximately 30 °C in the presence of carbon monoxide. However, another increase in toluene conversion was observed at around 150 °C with a maximum value of 25%. The best conversion at low temperature

could be explained by the exothermicity of the carbon monoxide total oxidation reaction (enthalpy to the CO total oxidation reaction ( $\Delta h$ ): -282 kJ mol<sup>-1</sup>). The oxidation of CO to  $\text{CO}_2$  is complete when toluene oxidation begins. CO oxidation can locally increases the catalyst bed temperature and allow activating the toluene oxidation reaction. Further evidence on toluene conversion is achieved via comparing the conversion curves with the chromatographic peak and MS analysis of water that should be formed during the toluene oxidation reaction. In this case, a similarity is observed, suggesting that the low temperature conversion is related to the oxidation of toluene and not toluene adsorption at the surface material (Fig. 7).

The presence of CO in the reaction mixture does not change the reactivity order of the catalysts. In addition, as previously observed during toluene oxidation in the absence of CO, the relationship between the reducibility and catalytic activity suggest a Mars Van Krevelen mechanism for the reaction. However, in this case, such mechanism has two options, namely, the model taking into account the competitive adsorption of reactant or not [5]. To get even deeper understanding on the toluene conversion at low temperature (150 °C) a further study was carried out to find out information on the by-product formation during oxidation of toluene in presence of CO

### 3.4. Identification of by products in total oxidation of toluene

To perform this study, a mass spectrometer (Omnistar Quadrupole Mass Spectrometer (QMS200) Pfeiffer-Vacuum) was coupled to the micro-GC and the CO and  $\text{CO}_2$  analyzers. The various by-products observed in the case of the toluene total oxidation on CoAlOMW and CoAlCeO catalysts are reported in Table 3.

Concerning the toluene total oxidation in absence of carbon monoxide, production of heavy by-products such as benzyl alcohol, benzaldehyde and benzene occurs at low conversion (< 20%). Regarding the lightest compounds (alkane and furan principally), their production takes place especially when the conversion is greater (> 20%). These by-products have already been reported in the literature [39,40].

Concerning the toluene total oxidation in presence of carbon monoxide, benzene, benzaldehyde, benzyl alcohol, methane and butane are also observed as by-product formed over both the catalysts. Production of benzaldehyde in this case could be taking place by the formation of peroxy carbonate species on the surface of the catalyst. The formation of these species occurs via the fixation of  $\text{CO}_2$  at the surface of the catalyst

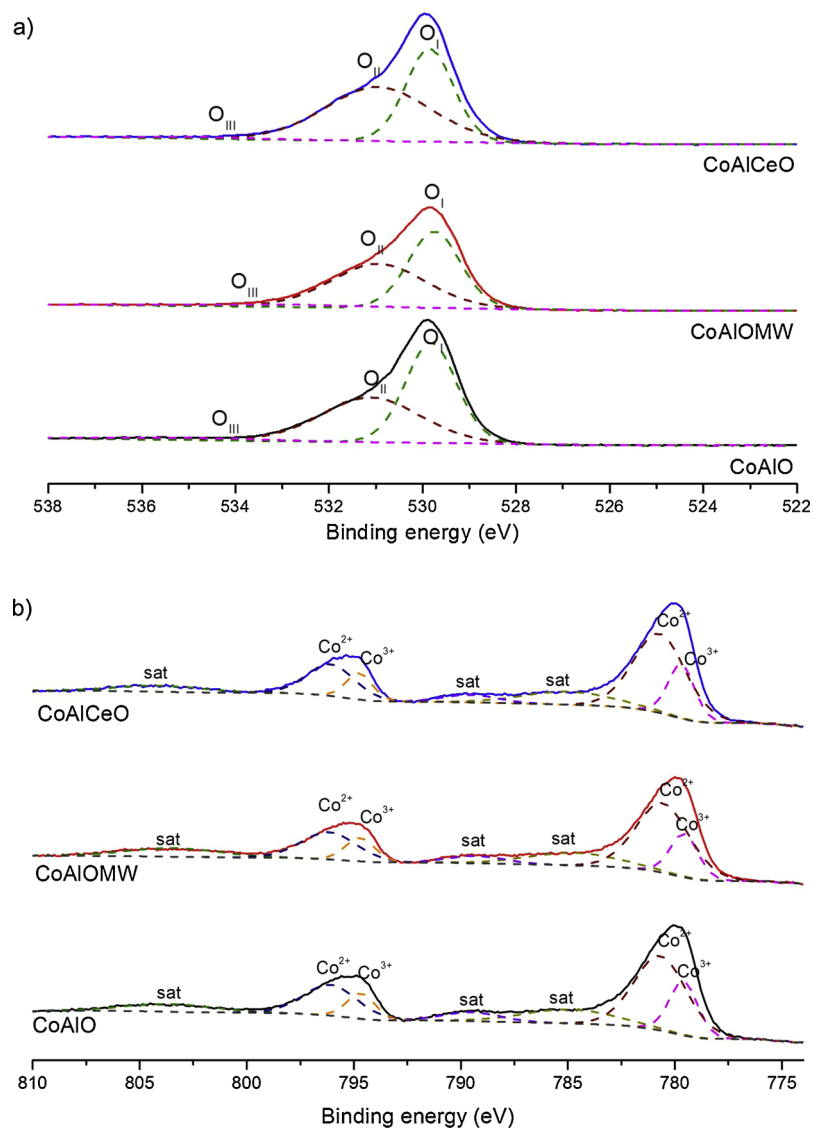


Fig. 4. XPS spectra of (a) O 1s and (b) Co 2p from the mixed oxides.

coming from CO oxidation reaction that takes place at lower temperature range. This carbon dioxide formed and adsorbed on the catalyst surface could react with oxygen present in the gas phase in order to form peroxy carbonate species on cobalt oxide [41]. At higher conversion ( $> 20\%$ ), presence of benzene, furan and butane indicates that the same mechanistic behavior than in the case of the toluene oxidation in absence of CO.

After observing the influence of carbon monoxide on the activity of various solids, a catalyst stability study for CoAlOMW and CoAlCeO was performed.

### 3.5. Catalyst stability for the two reactions

Stability tests in total oxidation of toluene are performed for the two catalysts (CoAlOMW and CoAlCeO) in presence and in absence of CO. Concerning the CoAlOMW mixed oxide, the stability test is conducted at 260 °C corresponding to a toluene initial conversion equal to 22% (Fig. 8). It is observed that toluene conversion oscillates between 20 and 26% with a period of about 24 h. The period change in toluene conversion can be explained by adsorption-desorption of the degradation products (by-products, CO<sub>2</sub>) on the catalyst surface. Tsou et al. [42] explain this type of oscillatory phenomenon by a reactive coke that is formed faster than it is oxidized and which start to accumulate on the

catalyst surface. At the end of aging test, the catalyst (CoAlOMW and CoAlCeO) has been studied by thermal analysis (DTA/TGA). This analysis shows no loss mass corresponding to the presence of coke. The absence of coke on the surface of the used catalyst allows us to consider that the oscillatory phenomenon can originate from the desorption of carbonate species (like CO<sub>2</sub>).

Concerning the CoAlCeO (Fig. 9), the test was conducted at 245 °C corresponding also to 22% of toluene conversion. The behavior of this catalyst is observed to be slightly different from the CoAlOMW. In fact, a slight increase in conversion was observed during the first hours of the test reaching 32% conversion, which is followed by deactivation during the following 20 h returning back to a conversion of 22%. The increase and decrease of the conversion continued during the duration of the test, but with a smaller decrease of conversion with an average value of 27%. The conversion was stable up to 95 h of testing and then increase in conversion was observed reaching the value of 55%. This increase is associated with a local increase (5 °C) of the catalyst temperature measured by the thermocouple placed on the catalyst bed (not shown). This local temperature increase is explained by the exothermicity of the toluene oxidation reaction (heat toluene combustion: 3739.8 kJ mol<sup>-1</sup>) [43]. Then, the toluene conversion returns to its value of approximately 30%. As in the case of the previous catalyst, oscillatory phenomenon is observed with a shorter period and less

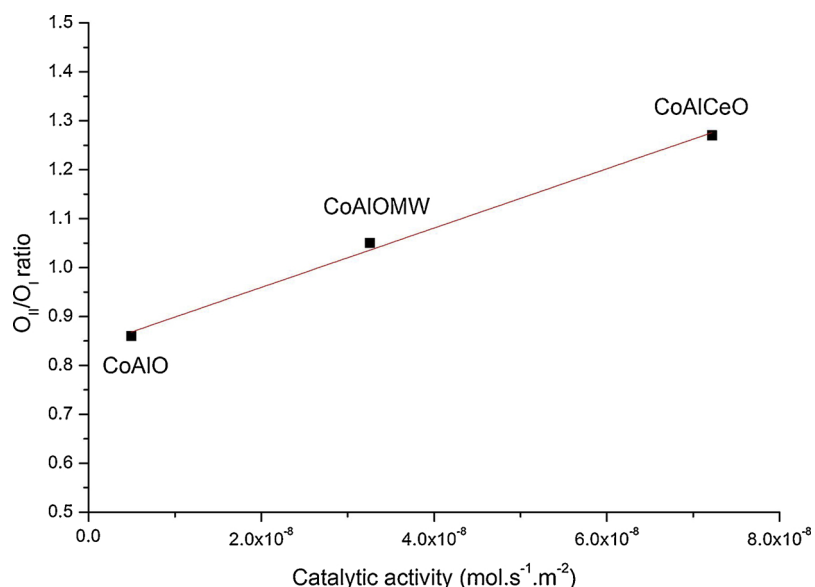


**Fig. 5.** Relation between catalytic activity measured at 241 °C corresponding to 20% of toluene conversion for CoAlCeO and the ratio  $O_{II}$  and  $O_I$  species calculated with XPS analysis.

intense oscillation than with CoAlOMW. To understand the oscillatory phenomenon and to evaluate the reducibility of the catalyst after the stability test, temperature programmed reduction was performed (Fig. 10). The profiles of the catalysts are similar to the profiles observed before test. This quite similar profile indicates that the reducibility of the catalyst was not modified during the stability test. However, despite the contribution of the catalyst reduction, an additional peak appears at 515 °C for CoAlOMW and at 510 °C for the CoAlCeO. This peak is attributed to  $\text{CO}_2$  desorption (identified by mass spectrometer analysis).

The stability test of the catalysts was also performed in presence of CO. This study was conducted at constant temperature corresponding to an initial conversion of toluene close to 20% with the feed of 1000 ppm of toluene and 1000 ppm of CO. The results are presented in Figs. 8 and 9.

For CoAlOMW catalyst, the stability test was conducted at 229 °C, while 201 °C for CoAlCeO. In the case of CoAlOMW catalyst it could be observed that the conversion increased at the beginning of the test (the three first hours of the test). After that the toluene conversion increases slightly during the duration of 150 h and reached 35% at the end of the test. For these studies, only the conversions of toluene are represented. The conversion of CO was quite stable during the entire stability test. This observation is also valid for the CoAlCeO catalysts.

The behavior of CoAlCeO was different. In fact, a slight increase in activity was observed during the first hours of the test reaching the conversion up to 26%. However, deactivation was observed during the following 20 h. At 20 h, the conversion returned to the initial level. After that, a stepwise increase of 4–5% of conversion is observed after every 20 h. This phenomenon reminds the oscillation observed during the stability test in the absence of CO. However, the amplitude of the

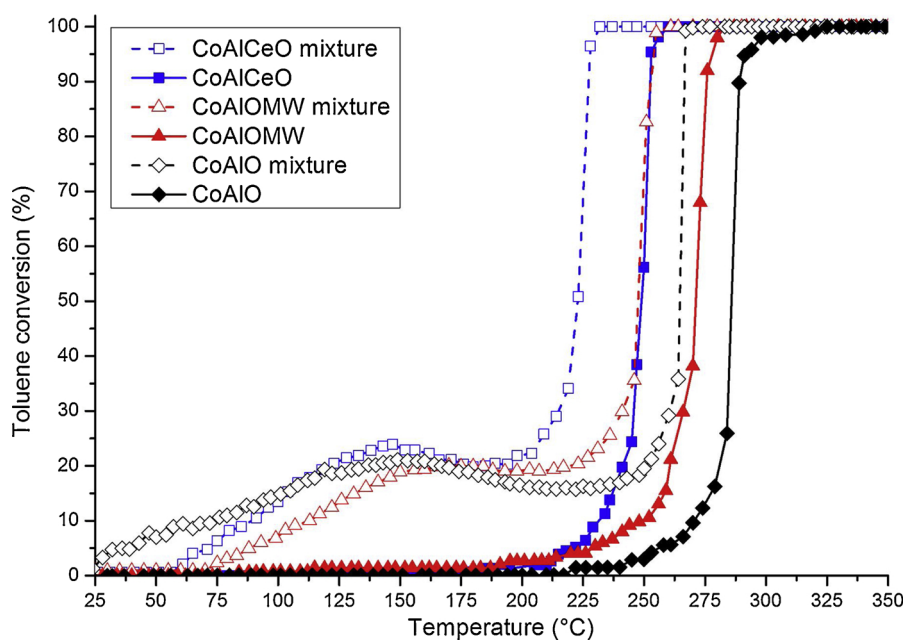


**Fig. 6.** Conversion of toluene (percentage) on mixed oxides vs. reaction temperature (°C) in presence of carbon monoxide in the gaseous mixture (solid line: in absence of CO; dashed line: in presence of CO).

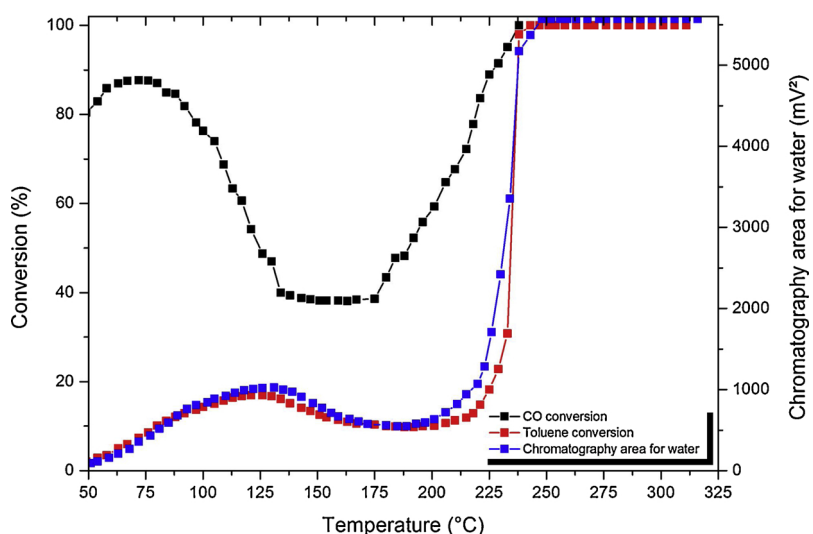


**Fig. 7.** Conversion of toluene and CO (percentage) on CoAlCeO mixed oxide vs. reaction temperature (°C) and water chromatography area vs. temperature during the CO-Toluene oxidation mixture.

**Table 3**

By-products analysed during the total oxidation of toluene in presence or absence of CO in the gaseous mixture.

Products	By-products observed			
	CoAlCeO		CoAlOMW	
	Without CO	With CO	Without CO	With CO
Toluene	X	X	X	X
Benzene	X	X	X	X
Benzaldehyde	X	X	X	X
Furan	X		X	X
Benzyl Alcohol	X	X		X
Pentadiene			X	X
Acid benzoic			X	X
Methane	X	X	X	X
Butane	X	X	X	X
Propane			X	X
CO <sub>2</sub>	X	X	X	X
CO	X	X	X	X

variation of the conversion was smaller in presence of CO. This can be explained by an amount of carbon dioxide or by-products adsorbed on the catalyst surface was lower in the case of the oxidation of toluene - CO. Indeed, the amount of available active sites for the toluene adsorption/oxidation is less since a part of these active sites are occupied for the CO total oxidation reaction. In general, it can be observed that addition of CO in toluene vapor increases the catalyst activity during the time. Furthermore, it demonstrates good stability of the developed materials in toluene.

#### 4. Conclusion

In this study, the activity of mixed oxides CoAl(Ce) prepared via hydroxide way in toluene total oxidation was studied in absence and presence of CO. Furthermore, the stability of CoAlCeO and CoAlOMW was tested during 150 h of time on stream.

An improvement of the activity of the three catalysts was observed when toluene was oxidized in presence of CO. This behaviour was most pronounced over CoAlCeO catalyst.

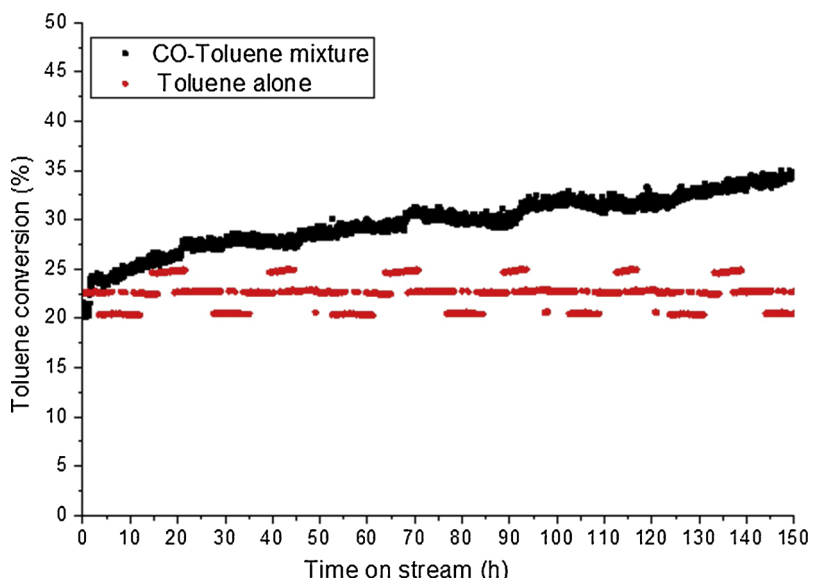


**Fig. 8.** Influence of time on stream on the conversion of toluene on the CoAlOMW catalyst in presence of CO (Black) or in absence of CO (Red) (For interpretation of the references to colour in this figure legend, the reader is referred to the web version of this article).

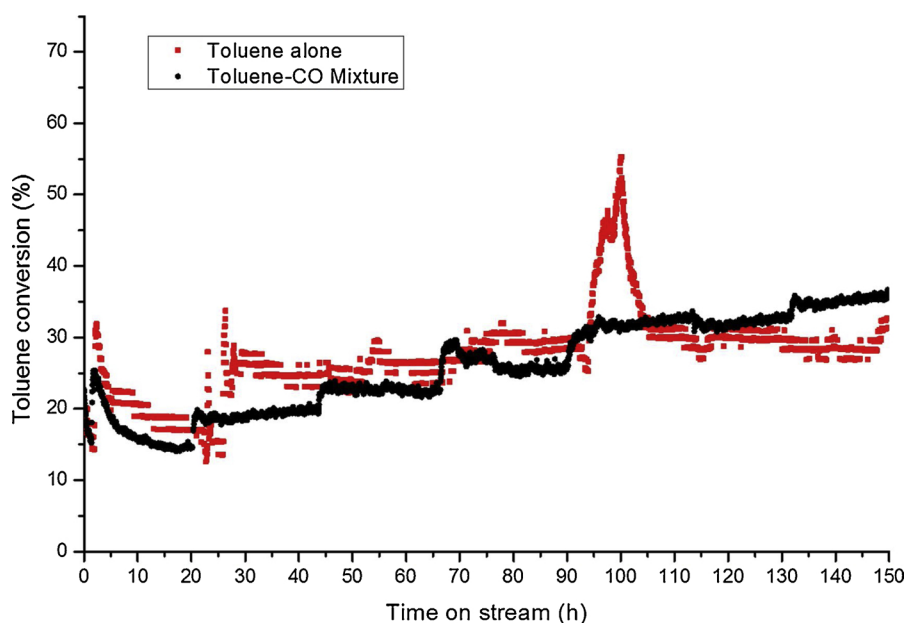


**Fig. 9.** Influence of time on stream on the conversion of toluene on the CoAlCeO catalyst in presence of CO (Black) or in absence of CO (Red) (For interpretation of the references to colour in this figure legend, the reader is referred to the web version of this article).

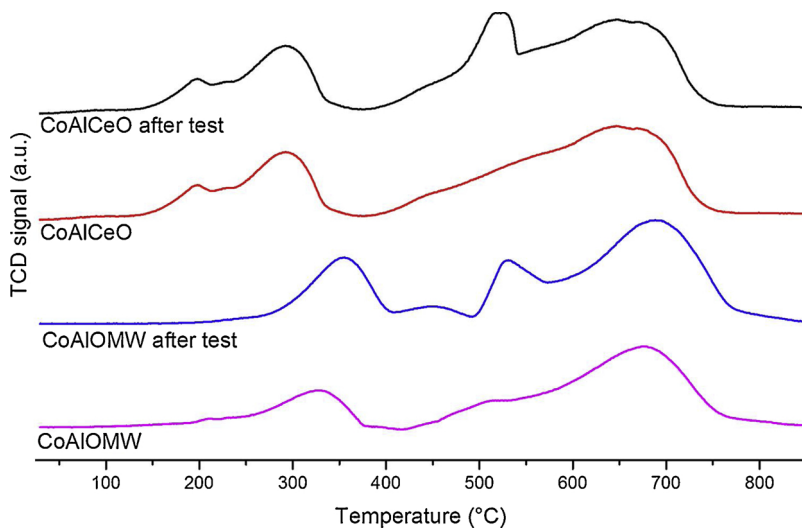


**Fig. 10.**  $\text{H}_2\text{-TPR}$  after aging test for CoAlCeO and CoAlOMW catalysts.

Based on hypothesis and observations, it was concluded that the improvement originates from the formation of by-products that are oxidized more easily than in absence of CO. The first by-product observed when the CO is present in the gaseous phase corresponds to the benzaldehyde while in case of toluene oxidation without CO; the first compound corresponds to benzylic alcohol. The latter one is more easily oxidized into  $\text{CO}_2$  and water than the toluene. Further analysis should be performed to confirm this observation.

During the stability tests in absence of CO an oscillatory behaviour was observed for CoAlOMW. After addition of Ce, the behaviour changed, however, certain periodicity remained. The periodic changes in toluene oxidation are due to the accumulation of  $\text{CO}_2$  or by-products on the catalytic material during the stability test. After a period, the desorption and the oxidation of by-products takes place and the catalyst surface is empty to begin a new catalytic cycle.

These results demonstrate the good activity and stability of CoAl (Ce) based catalysts in toluene total oxidation, with or without carbon monoxide in the gaseous flow.

## Acknowledgements

Authors want to acknowledge the “Agency of Environment and Energy Management” (ADEME) as well as Nord-Pas-de-Calais region for the funding of the work. Authors also acknowledge the “Centre Commun de Mesure” of the University Littoral Côte d’Opale.

## References

- [1] S. Ojala, N. Koivikko, T. Laitinen, A. Mouammine, P. Seelam, S. Laassiri, K. Ainassaari, R. Brahma, R. Keiski, Utilization of volatile organic compounds as an alternative for destructive abatement, *Catalysts* 5 (2015) 1092–1151, <https://doi.org/10.3390/catal5031092>.
- [2] S. Scirè, L.F. Liotta, Supported gold catalysts for the total oxidation of volatile organic compounds, *Appl. Catal. B Environ.* 125 (2012) 222–246, <https://doi.org/10.1016/j.apcatb.2012.05.047>.
- [3] S. Ivanova, C. Petit, V. Pitchon, Application of heterogeneous gold catalysis with increased durability: oxidation of CO and hydrocarbons at low temperature, *Gold Bull.* 39 (2006) 3–8 (Accessed 1 March 2013), <http://www.springerlink.com/index/LW1054176N358066.pdf>.
- [4] T. Ataloglou, J. Vakros, K. Bourikas, C. Fountzoula, C. Kordulis, A. Lycourghiotis,

Influence of the preparation method on the structure–activity of cobalt oxide catalysts supported on alumina for complete benzene oxidation, *Appl. Catal. B Environ.* 57 (2005) 299–312, <https://doi.org/10.1016/j.apcatb.2004.11.010>.

[5] M. Baldi, V.S. Escribano, J.M.G. Amores, F. Milella, G. Busca, Characterization of manganese and iron oxides as combustion catalysts for propane and propene, *Appl. Catal. B Environ.* 17 (1998) L175–L182, [https://doi.org/10.1016/S0926-3373\(98\)00013-7](https://doi.org/10.1016/S0926-3373(98)00013-7).

[6] S.C. Kim, W.G. Shim, Catalytic combustion of VOCs over a series of manganese oxide catalysts, *Appl. Catal. B Environ.* 98 (2010) 180–185, <https://doi.org/10.1016/j.apcatb.2010.05.027>.

[7] A. Trovarelli, *Catalysis by Ceria and Related Materials*, Imperial C, World Scientific Publishing Company, 2002.

[8] W. Gao, Y. Zhao, J. Liu, Q. Huang, S. He, C. Li, J. Zhao, M. Wei, Catalytic conversion of syngas to mixed alcohols over CuFe-based catalysts derived from layered double hydroxides, *Catal. Sci. Technol.* 3 (2013) 1324, <https://doi.org/10.1039/c3cy00025g>.

[9] L.F. Liotta, M. Ousmane, G. Di Carlo, G. Pantaleo, G. Deganello, A. Boreave, A. Giroir-Fendler, Catalytic removal of toluene over  $\text{Co}_3\text{O}_4\text{-CeO}_2$  mixed oxide catalysts: comparison with  $\text{Pt}/\text{Al}_2\text{O}_3$ , *Catal. Lett.* 127 (2008) 270–276, <https://doi.org/10.1007/s10562-008-9640-0>.

[10] E. Genty, L. Jacobs, T. Visart De Bocarmé, C. Barroo, Dynamic processes on gold-based catalysts followed by environmental microscopies, *Catalysts* 134 (2017) 1–44, <https://doi.org/10.3390/catal7050134>.

[11] K. Jiratova, P. Cuba, F. Kovanda, L. Hilaire, V. Pitchon, Preparation and characterisation of activated Ni (Mn)/ Mg / Al hydrotalcites for combustion catalysis, *Catal. Today* 76 (2002) 43–53.

[12] E. Genty, R. Cousin, S. Capelle, C. Gennequin, S. Siffert, Catalytic oxidation of toluene and CO over nanocatalysts derived from hydrotalcite-like compounds ( $\text{X}_{\text{x}}^{2+}\text{Al}_{\text{x}}^{3+}$ ): effect of the bivalent cation, *Eur. J. Inorg. Chem.* 2012 (2012) 2802–2811, <https://doi.org/10.1002/ejic.201101236>.

[13] C. Gennequin, S. Siffert, R. Cousin, A. Aboukaïs, Co-Mg-Al hydrotalcite precursors for catalytic total oxidation of volatile organic compounds, *Top. Catal.* 52 (2009) 482–491, <https://doi.org/10.1007/s11244-009-9183-7>.

[14] C.-W. Tang, M.-C. Kuo, C.-J. Lin, C.-B. Wang, S.-H. Chien, Evaluation of carbon monoxide oxidation over  $\text{CeO}_2/\text{Co}_3\text{O}_4$  catalysts: effect of ceria loading, *Catal. Today* 131 (2008) 520–525, <https://doi.org/10.1016/j.cattod.2007.10.026>.

[15] D.P. Debecker, E.M. Gaigneaux, G. Busca, Exploring, tuning, and exploiting the basicity of hydrotalcites for applications in heterogeneous catalysis, *Chemistry* 15 (2009) 3920–3935, <https://doi.org/10.1002/chem.200900060>.

[16] C.-T. Chang, B.-J. Liaw, C.-T. Huang, Y.-Z. Chen, Preparation of  $\text{Au}/\text{Mg-AlO}$  hydrotalcite catalysts for CO oxidation, *Appl. Catal. A Gen.* 332 (2007) 216–224, <https://doi.org/10.1016/j.apcata.2007.08.021>.

[17] L. A Palacio, J. Velásquez, A. Echavarría, A. Faro, F.R. Ribeiro, M.F. Ribeiro, Total oxidation of toluene over calcined trimetallic hydrotalcites type catalysts, *J. Hazard. Mater.* 177 (2010) 407–413, <https://doi.org/10.1016/j.jhazmat.2009.12.048>.

[18] L.A. Palacio, J.M. Silva, F.R. Ribeiro, M.F. Ribeiro, Catalytic oxidation of volatile organic compounds with a new precursor type copper vanadate, *Catal. Today* 133–135 (2008) 502–508, <https://doi.org/10.1016/j.cattod.2007.12.015>.

[19] S. Tanasoi, G. Mitran, N. Tanchoux, T. Cacciaguerra, F. Fajula, I. Săndulescu, D. Tichit, I.-C. Marcu, Transition metal-containing mixed oxides catalysts derived from LDH precursors for short-chain hydrocarbons oxidation, *Appl. Catal. A Gen.* 395 (2011) 78–86, <https://doi.org/10.1016/j.apcata.2011.01.028>.

[20] J. Carpentier, S. Siffert, J.F. Lamonié, H. Laversin, a. Aboukaïs, Synthesis and characterization of Cu–Co–Fe hydrotalcites and their calcined products, *J. Porous Mater.* 14 (2006) 103–110, <https://doi.org/10.1007/s10934-006-9014-1>.

[21] J. Carpentier, J.F. Lamonié, S. Siffert, E.A. Zhilinskaya, A. Aboukaïs, Characterisation of Mg / Al hydrotalcite with interlayer palladium complex for catalytic oxidation of toluene, *Appl. Catal. A Gen.* 234 (2002) 91–101.

[22] L.F. Liotta, H. Wu, G. Pantaleo, A.M. Venezia,  $\text{Co}_3\text{O}_4$  nanocrystals and  $\text{Co}_3\text{O}_4\text{-MO}_x$  binary oxides for CO,  $\text{CH}_4$ , and VOC oxidation at low temperatures: a review, *Catal. Sci. Technol.* 3 (2013) 3085, <https://doi.org/10.1039/c3cy00193h>.

[23] K. Jirátová, J. Mikulová, J. Klempa, T. Grygar, Z. Bastl, F. Kovanda, Modification of Co–Mn–Al mixed oxide with potassium and its effect on deep oxidation of VOC, *Appl. Catal. A Gen.* 361 (2009) 106–116, <https://doi.org/10.1016/j.apcata.2009.04.004>.

[24] M. Gabrovská, R. Edreva-Kardjieva, K. Tenchev, P. Tzvetkov, A. Spojakina, L. Petrov, Effect of Co-content on the structure and activity of Co–Al hydrotalcite-like materials as catalyst precursors for CO oxidation, *Appl. Catal. A Gen.* 399 (2011) 242–251, <https://doi.org/10.1016/j.apcata.2011.04.007>.

[25] J. Pérez-Ramírez, G. Mul, J.A. Moulijn, In situ Fourier transform infrared and laser Raman spectroscopic study of the thermal decomposition of  $\text{Co} \pm \text{Al}$  and  $\text{Ni} \pm \text{Al}$  hydrotalcites, *Vib. Spectrosc.* 27 (2001) 75–88.

[26] L.F. Liotta, G. Di Carlo, G. Pantaleo, A.M. Venezia, G. Deganello,  $\text{Co}_3\text{O}_4\text{/CeO}_2$  composite oxides for methane emissions abatement: Relationship between  $\text{Co}_3\text{O}_4\text{-CeO}_2$  interaction and catalytic activity, *Appl. Catal. B Environ.* 66 (2006) 217–227, <https://doi.org/10.1016/j.apcatb.2006.03.018>.

[27] E. Genty, R. Cousin, C. Gennequin, S. Capelle, A. Aboukaïs, S. Siffert, Investigation of Au/hydrotalcite catalysts for toluene total oxidation, *Catal. Today* 176 (2011) 116–119, <https://doi.org/10.1016/j.cattod.2011.01.034>.

[28] E. Genty, J. Brunet, R. Pequeux, S. Capelle, S. Siffert, R. Cousin, Effect of Ce substituted hydrotalcite-derived mixed oxides on total catalytic oxidation of air pollutant, *Mater. Today Proc.* 3 (2016) 277–281, <https://doi.org/10.1016/j.matpr.2016.01.069>.

[29] E. Genty, J. Brunet, C. Poupin, S. Casale, S. Capelle, P. Massiani, S. Siffert, R. Cousin, Co-Al mixed oxides prepared via LDH route using microwaves or ultrasound: application for catalytic toluene total oxidation, *Catalysts* 5 (2015) 851–867, <https://doi.org/10.3390/catal5020851>.

[30] E. Genty, S. Siffert, R. Cousin, Investigation of reaction mechanism and kinetic modelling for the toluene total oxidation in presence of CoAlCe catalyst, *Catal. Today* (2018) 1–8, <https://doi.org/10.1016/j.cattod.2018.03.018>.

[31] B. Grbic, N. Radic, A. Terlecki-Barcivic, Kinetics of deep oxidation of n-hexane and toluene over Pt/Al<sub>2</sub>O<sub>3</sub> catalysts, *Appl. Catal. B Environ.* 50 (2004) 161–166, <https://doi.org/10.1016/j.apcatb.2004.01.012>.

[32] J. Brunet, E. Genty, C. Barroo, F. Cazier, C. Poupin, S. Siffert, D. Thomas, G. De Weireld, T.V. de Bocarmé, R. Cousin, The CoAlCeO mixed oxide: an alternative to palladium-based catalysts for total oxidation of industrial VOCs, *Catalysts* 8 (2018), <https://doi.org/10.3390/catal8020064>.

[33] G. Fetter, F. Hernández, A. Maubert, Microwave irradiation effect on hydrotalcite synthesis, *J. Porous Mater.* 30 (1997) 27–30 (Accessed 12 April 2013), <http://link.springer.com/article/10.1023/A%3A100961900529>.

[34] Y. Liu, H. Dai, J. Deng, S. Xie, H. Yang, W. Tan, W. Han, Y. Jiang, G. Guo, Mesoporous  $\text{Co}_3\text{O}_4$ -supported gold nanocatalysts: highly active for the oxidation of carbon monoxide, benzene, toluene, and o-xylene, *J. Catal.* 309 (2014) 408–418, <https://doi.org/10.1016/j.jcat.2013.10.019>.

[35] J.-C. Dupin, D. Gonbeau, P. Vinatier, A. Levasseur, Systematic XPS studies of metal oxides, hydroxides and peroxides, *Phys. Chem. Chem. Phys.* 2 (2000) 1319–1324.

[36] D. Delimaris, T. Ioannides, VOC oxidation over MnO<sub>x</sub>–CeO<sub>2</sub> catalysts prepared by a combustion method, *Appl. Catal. B Environ.* 84 (2008) 303–312, <https://doi.org/10.1016/j.apcatb.2008.04.006>.

[37] J.T. Sampanthar, H.C. Zeng, Synthesis of  $\text{Co}^{II}\text{Co}^{III}_{2-x}\text{Al}_x\text{O}_4\text{-Al}_2\text{O}_3$  nanocomposites via sol-gel  $\gamma\text{-Al}_2\text{O}_3$  matrix, *Chem. Mater.* 13 (2001) 4722–4730.

[38] T. Garcia, S. Agouram, J.F. Sánchez-Royo, R. Murillo, A.M. Mastral, A. Aranda, I. Vázquez, A. Dejoz, B. Solsona, Deep oxidation of volatile organic compounds using ordered cobalt oxides prepared by a nanocasting route, *Appl. Catal. A Gen.* 386 (2010) 16–27, <https://doi.org/10.1016/j.apcata.2010.07.018>.

[39] S. Lars, T. Andersson, Reaction networks in the catalytic vapor-phase oxidation of toluene and xylenes, *J. Catal.* 98 (1986) 138–149.

[40] J. Brunet, E. Genty, Y. Landkoc, M. Al Zallouha, S. Billet, D. Courcot, S. Siffert, D. Thomas, G. De Weireld, R. Cousin, Identification of by-products issued from the catalytic oxidation of toluene by chemical and biological methods, *Comptes Rendus Chim.* 18 (2015) 1084–1093, <https://doi.org/10.1016/j.crci.2015.09.001>.

[41] G. Centi, P. Lanzafame, S. Perathoner, Performances of Co-based catalysts for the selective side chain oxidation of toluene in the gas phase, *Catal. Today* 99 (2005) 161–170, <https://doi.org/10.1016/j.cattod.2004.09.036>.

[42] J. Tsou, P. Magnoux, M. Guisnet, J.J.M. Orfao, J.L. Figueiredo, Oscillations in the catalytic oxidation of volatile organic compounds, *J. Catal.* 225 (2004) 147–154, <https://doi.org/10.1016/j.jcat.2004.03.045>.

[43] A.A. Barassi, G. Baldi, Deep catalytic oxidation of aromatic hydrocarbon mixtures: reciprocal inhibition effects and kinetics, *Ind. Eng. Chem. Res.* 33 (1994) 2964–2974.